09

Quantum cascade detectors for the 8 μm spectral range

© V.V. Dudelev[1], D.V. Chistyakov[1], V.V. Podoprigora[1,2], A.A. Nikitin[1,2], D.A. Mikhailov[1], E.D. Cherotchenko[1], I.I. Vrubel[1], V.Yu. Mylnikov[1], S.N. Losev[1], N.G. Deryagin[1], S.Kh. Abdulrazak[1], A.D. Andreev[1], A.G. Deryagin[1], A.V. Babichev[1], A.V. Lutetskiy[1], S.O. Slipchenko[1], N.A. Pikhtin[1], A.G. Gladyshev[3], K.A. Podgaetskiy[4], A.Yu. Andreev[4], I.V. Yarotskaya[4], M.A. Ladugin[4], A.A. Marmalyuk[4], D.S. Papylev[5], I.I. Novikov[3,5], E.A. Kognovitskaya[1,6], V.I. Kuchinskii[1], L.Ya. Karachinsky[3,5], A.Yu. Egorov[3], G.S. Sokolovskii[1]

[1] Ioffe Institute, St. Petersburg, Russia
[2] St. Petersburg State Electrotechnical University „LETI“, St. Petersburg, Russia
[3] Connector Optics LLC, St. Petersburg, Russia
[4] JSC „M.F. Stelmakh Research Institute Polyus“ Moscow, Russia
[5] ITMO University, St. Petersburg, Russia
[6] D.I. Mendeleev Institute for Metrology, St. Petersburg, Russia
E-mail: v.dudelev@mail.ru

Received November 1, 2025
Revised December 9, 2025
Accepted December 9, 2025

Quantum cascade detectors (QCDs) operating at room temperature and zero bias with extremely low dark current are a promising platform for creating high-speed detectors in the long-wave infrared range for wireless optical communication systems. Producing QCDs from the quantum cascade laser (QCL) heterostructures opens up opportunities for integrating sources and detectors on a common wafer. We have demonstrated a maximum QCD sensitivity of over 70 mA/W in the 8 μm region and implemented the concept of integrating QCD on a single heat sink with QCL to create a feedback photodetector. Preliminary performance studies have shown that the QCD bandwidth exceeds 1 GHz and may be significantly increased by optimizing the capacitive characteristics.

Keywords: quantum cascade detector, quantum cascade laser, feedback photodetector, bandwidth.

DOI: 10.61011/TPL.2026.04.63203.20555

Mid-infrared (IR) photonics attracts increasing attention due to the existence in the mid-IR range of a large number of intense absorption lines of various substances , as well as of atmospheric transparency windows. These unique properties of the mid-IR range are of great practical importance as they open up significant prospects for developing various applications related to spectroscopy and also for developing noise-immune wireless optical communication lines.

Development of applied areas of mid-IR photonics needs creating both efficient emitters and photodetectors. At present, the most efficient mid-IR laser emitters are quantum cascade lasers (QCLs) which emit watts of optical power at room temperature [1,2] and are successfully used both in spectroscopy for identifying various substances [3] (among others, in biomedical applications [4]) and also for transmitting information through wireless optical communication lines [5].

At the same time, operation of such systems needs not only light sources but also efficient and, in the case of communication systems, high-speed detectors. Conventional approaches imply the use of photodetectors based on mercury-cadmium-tellurium (MCT) compounds [6], detectors based on type-II superlattices InAs/InAsSb (T2SL) [7], and detectors based on GaAs/AlGaAs superlattices (QWIPs) [8]. MCT detectors exhibit quite high sensitivity but require additional cooling, which significantly reduces their compactness and increases energy consumption. In addition, operation speed of up-to-date MCT detectors is restricted to 1 GHz. T2SL detectors exhibit room-temperature operation speed exceeding 10 GHz at the wavelength of 4.5 μm [7]. As their disadvantages, we may consider the limited spectral range available for these detectors (< 6, μm) and high room-temperature dark current which reduces the ability to detect relatively weak signals. QWIP detectors have demonstrated very a high operation speed (above 100 GHz for the $\sim 10\,\mu$m wavelength at room temperature [8]); however, in the absence of cooling QWIP detectors have very high leakage currents, which reduces detectability of such devices.

An alternative approach is the use of quantum cascade detectors (QCDs). QCD is a unipolar device operating on electron transitions between the conduction-band quantum levels rather than on interband transitions like, e. g., photodiodes. Similar to the QCL structure, that of QCD consists of dozens of quantum cascades; in each of them, a photon is absorbed, which ensures electron excitation from the lower level to upper one with successive diagonal relaxation down in energy between the levels of adjacent quantum wells in the transport zone. Thus, the electron transits from one cascade to another (Fig. 1). By now, QCDs have been created for the 4.5 μm spectral range with a cutoff frequency of more than 20 GHz [9]; it has been theoretically shown that the cutoff frequency may exceed 100 GHz [10].

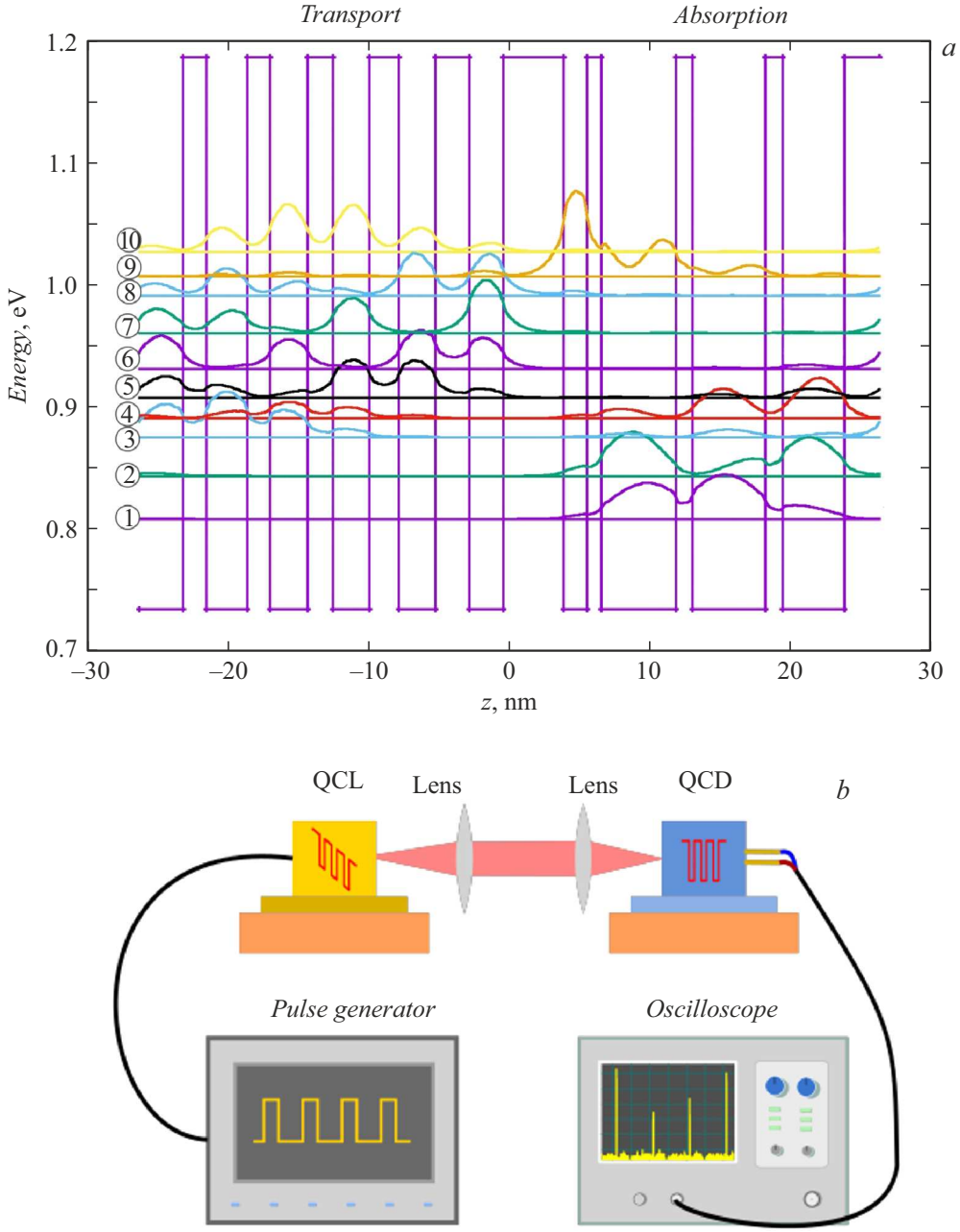

Figure 1. *a* — QCD band diagram; *b* — schematic representation of the setup for studying QCD characteristics.

In addition, detection of femtosecond pulses has been demonstrated [11]. The possibility of creating high-speed QCDs with the bandwidth of > 20 GHz for the long-wave infrared range was demonstrated for a design comprising an antenna amplifier [12]. Another QCD advantage is the possibility of its integration with QCL; this was clearly demonstrated in [13]. This fact is one of the main QCD advantages, since it opens up the possibility of creating photonic integrated circuits for practical applications which are not only optical communications, but also heterodyne detection and mid-IR spectroscopy. Therewith, for successful QCL-QCD integration on a common platform, it is preferable that either both devices be manufactured based on the same heterostructure to obtain homogeneous integration or have the same thickness of the waveguide core and upper waveguide cladding to obtain heterogeneous integration. The goal of this study was to develop and create long-wave IR high-speed detectors for wireless optical communications and gas analysis systems, which would be able to be integrated with quantum cascade lasers on a common platform.

In this work, we have investigated QCDs in the classical waveguide geometry for detecting radiation of about $8\,\mu$m. Fig. 1, *a* presents the energy band diagram of

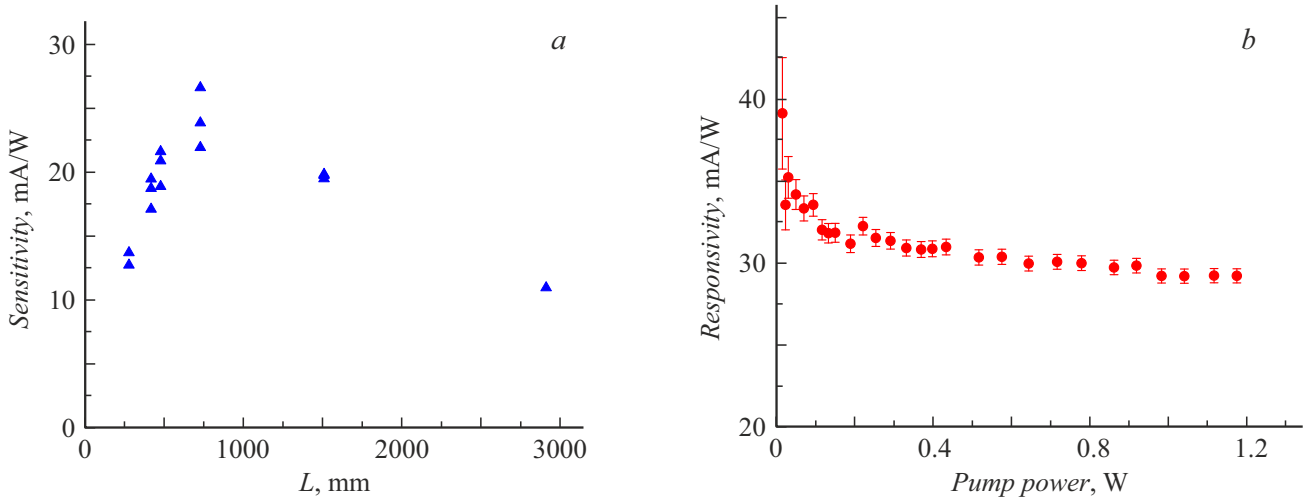

Figure 2. Results of studying the QCD sensitivity dependence on the chip length at a detected power higher than 1.5 W (*a*) and on the pump power for a QCD 700 μm long (*b*).

the QCD quantum cascade; the absorption and transport zones are marked. QCDs were fabricated based on QCL heterostructures with 50 quantum cascades in the active region, which are described in [1,2]. Thickness of the active region consisting of InGaAs/InAlAs layers matched with the InP substrate was 2.5 μm, while the total waveguide-core thickness embracing the active region and lower InGaAs buffer layer 100 nm thick was 2.6 μm. The waveguide claddings consisted of indium phosphide. In experiments, both stripe QCDs with the stripe width of 40 μm and four-cleavage samples $\sim 0.1\,\text{mm}^2$ in area were used. Input facets of all the samples were made by cleaving along the crystallographic axes. No anti-reflective coating was applied. Stripe QCDs were fabricated similarly to QCLs under the procedure of post-growth treatment described in [14].

The QCD sensitivity dependence on the chip length was studied on a set of samples 0.25 to 3 mm long. Pumping was performed by using QCL with the generation wavelength of $\sim 7.6\,\mu$m. QCL operated in the pulsed generation mode under pumping with current pulses ~ 100 ns in length and 10 kHz in repetition rate. The pump pulse power was 1.75 W.

Fig. 1, *b* schematically represents the experimental setup. The QCL radiation was collected by an aspherical lens with a broadband antireflective coating. Reflectivities of the lens surfaces were below 1 %. The lens numerical aperture was NA = 0.56. QCL radiation was introduced into the QCD waveguide with the aid of an identical lens. QCD, QCL and lenses were secured on high-precision positioners with differential micrometer screws. The QCL-to-QCD distance was ~ 30 cm. The results of studying the QCD sensitivity dependence on the chip length are presented in Fig. 2, *a*. The maximum sensitivity was obtained for QCD 0.7 mm long and amounted to ~ 27 mA/W. This estimate of sensitivity accounts for the Fresnel loss by reflection from the QCD input facet but ignores the radiation loss by introduction into the QCD waveguide. Actually, here is presented the instrumental sensitivity for the optical system configuration suitable for practical application. The focal spot size for an ideal Gaussian beam at the $1/e$ level for the used lens with numerical aperture NA = 0.56 is $w_0 = \lambda/(\pi \cdot \text{NA}) \approx 4.5\,\mu$m. In this case, the realistic value of the QCL beam propagation parameter M^2 along the fast axis is at least 1.2. The M^2 effect comes to a proportional increase in the focal spot size: $w_0 \to M^2 w_0$. Then, neglecting the slow-axis divergence, obtain that the radiation fraction introduced into the waveguide by the optical system does not exceed 50 %, which should be taken into account in calculating the maximum sensitivity.

Studies of the QCD sensitivity have shown that it remains almost constant at pump powers of about 0.1 W and higher. While the power to be detected continues decreasing, an increase in sensitivity is observed (Fig. 2, *b*). Data presented in [13] shows that the QCD sensitivity saturation is also observed with increasing power under detection. For QCDs we examine, the detected power of about 0.1 W is, apparently, the saturation power. Therefore, a considerable increase in sensitivity is observed at radiation powers below this value. If the experimentally obtained sensitivity is normalized to the ratio between the active region thickness and focal spot size, and chip length is optimal, the maximum sensitivity exceeds 50 mA/W at a watt-level detected power and 70 mA/W at the detected power of about 10 mW. If the power to be detected is reduced to the microwatt level and normalized to the thickness of a single quantum cascade (as in [15]), a further increase in the maximum QCD sensitivity may be expected.

The non-monotonic dependence of QCD sensitivity on the chip length (Fig. 2, *a*) is associated with its increase due to an increase in the fraction of absorbed radiation at short lengths and decrease due to signal shunting because of an internal resistance decrease at chip lengths significantly

exceeding the absorption length:

$$S = S_0 \frac{1 - \exp(-\alpha L)}{1 + RWL/\rho}, \qquad (1)$$

where S_0 is the maximum sensitivity, L is the chip length, W is the chip width, R is the external resistance, ρ is the chip resistivity, α is the absorption coefficient.

Note that the demonstrated sensitivity is quite sufficient for solving applied problems. One possible solution is to use QCD as a feedback photodetector for QCL. Using QCDs made from the same structure as QCLs allows avoiding problems with height adjustment during installation. Mounting QCD at the distance of 30–100 μm from QCL, it is possible to obtain a sufficient input factor for calibrating the laser output power. We have prepared QCL samples mounted on the common heat sink with QCD having a four-cleavage configuration $\sim 200 \times 500\,\mu$m in dimensions. Since the laser stripe size was 20 μm, selection of this configuration made unnecessary precise alignment both vertically and in the heat sink plane. Both QCD and QCL were mounted with the epitaxial layer down, which ensured automatic fast-axis alignment. A photo of the installed feedback QCL–QCD pair is given in the inset to Fig. 3, *b*. Evidently, QCD is located at a distance significantly less than 100 μm from the QCL rear mirror (the QCL chip width is 400 μm).

Fig. 3, *a* shows the QCL volt-ampere characteristic (curve *1*) and watt-ampere characteristics measured with the external photodetector (curve *2*) and QCD integrated with QCL on a common heat sink (dots). One can see that shapes of both watt-ampere characteristics match well. The total feedback QCD sensitivity is slightly lower than 3 mA/W (Fig. 3, *b*), which is because of a decrease in the chip internal resistance due to an increase in the active region (1) width; however, it is quite sufficient for controlling the QCL power based on its readings.

As already noted, long-IR QCDs are important for wireless optical communication systems. Fig. 4 presents a track of pulses recorded using QCD pulses less than 20 ns in duration and 10 MHz in repetition rate. It is clear that in this configuration there may be realized a stable wireless optical communication with the data transmission rate of 10 Mb/s which is limited only by capabilities of the QCL electrical pumping circuit.

To refine the maximum response time of QCDs under consideration, we have studied detection of optical radiation with QCL $300 \times 300\,\mu$m in size pumped by subnanosecond current pulses. The QCL radiation beam was split into two parts in the 9:1 ratio between QCL and high-speed MTC photodetector Vigo PVI-4TE-10.6-1x1 with four-stage cooling and 1 GHz bandwidth. Both photodetectors were connected to real-time oscilloscope Rigol DS70504 with the bandwidth of 5 GHz.

As shown in Fig. 4, *b*, duration of the photo-response pulse detected by QCD is not inferior to that of the high-speed CMT photodetector and does not exceed ~ 0.8 ns. Note here that sensitivity of the reference MTC receiver is significantly higher than that of the studied QCDs, because, among other factors, a high-speed amplifier is used. At the same time, the achieved result shows that even without optimizing the QCD design and installation techniques aimed at reducing the device capacitance and inductance, the QCD bandwidth exceeds 1 GHz. This allows us to expect applicability of such photodetectors in wireless optical communication systems with the data transmission speeds of 1 Gb/s and higher.

Thus, this paper presents the results of studying the 8 μm QCDs. The study has shown the fact that the maximum QCD sensitivity exceeds 70 mA/W in the vicinity of 8 μm, and also the potential for implementing wireless optical data transmission lines with the rates of approximately 1 Gb/s. Further research into QCDs will be aimed at increasing their performance by optimizing the QCD chip design and mounting it so as to reduce its electrical capacitance; the research will be also devoted to developing the ideas for integrating QCL and QCD on a common platform

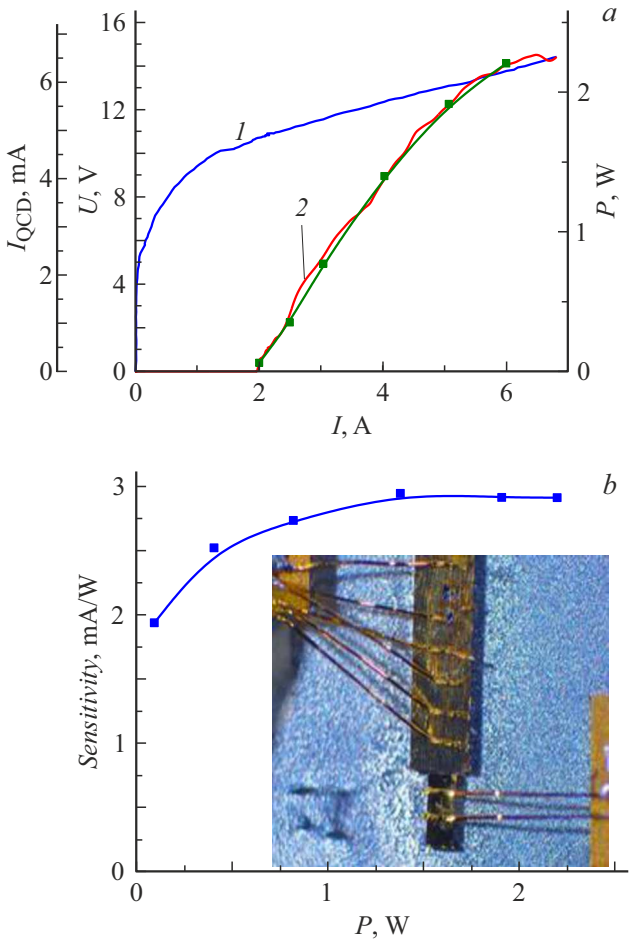

Figure 3. *a* — the QCL volt-ampere (curve *1*) and watt-ampere characteristics. Curve *2* is the watt-ampere characteristic measured on a computer-aided setup. Dots represent the measurements obtained by using a feedback QCD (axis I_{QCD}). *b* — dependence of the feedback QCD sensitivity on the QCL power. The inset shows a photograph of the QCL–feedback QCD pair.

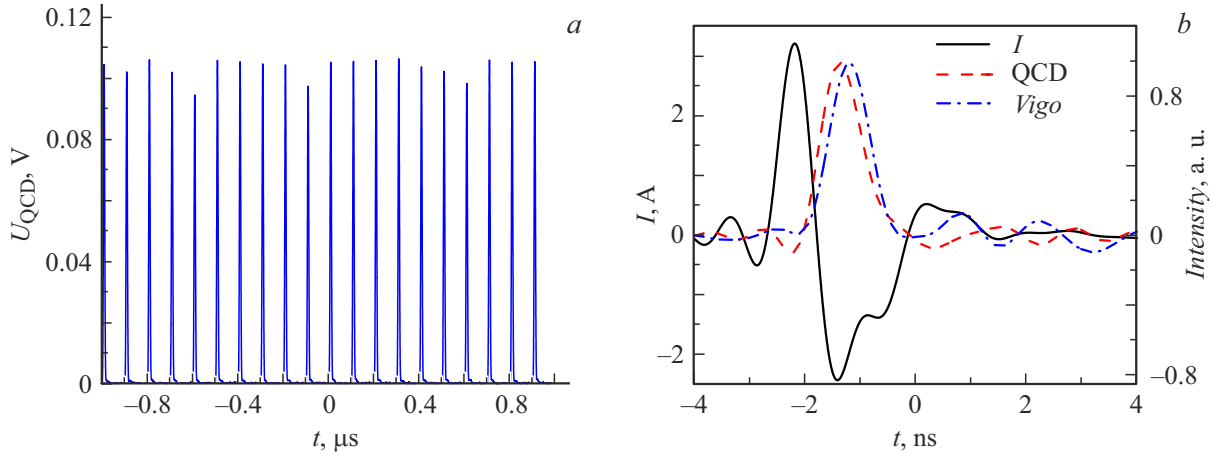

Figure 4. *a* — a track of pulses 10 MHz in repetition rate emitted by QCL and recorded by QCD. *b* — measurements of radiation of QCL pumped by subnanosecond current pulses. The solid curve represents the current through the laser, dashed line is for the radiation detected by QCD, dash-dotted line is the radiation detected by the MCT photodetector.

for the purpose of expanding the range of their possible applications.

Funding

The study was supported by the Russian Science Foundation, project No 21-72-30020-P (https://rscf.ru/project/21-72-30020/).

Conflict of interests

The authors declare that they have no conflict of interests.

References

[1] E. Cherotchenko, V. Dudelev, D. Mikhailov, G. Savchenko, D. Chistyakov, S. Losev, A. Babichev, A. Gladyshev, I. Novikov, A. Lutetskiy, D. Veselov, S. Slipchenko, D. Denisov, A. Andreev, I. Yarotskaya, K. Podgaetskiy, M. Ladugin, A. Marmalyuk, N. Pikhtin, L. Karachinsky, V. Kuchinskii, A. Egorov, G. Sokolovskii, Nanomaterials, **12**, 3971 (2022). DOI: 10.3390/nano12223971

[2] V.V. Dudelev, E.D. Cherotchenko, I.I. Vrubel, D.A. Mikhailov, D.V. Chistyakov, V.Yu. Mylnikov, S.N. Losev, E.A. Kognovitskaya, A.V. Babichev, A.V. Lutetskiy, S.O. Slipchenko, N.A. Pikhtin, A.V. Abramov, A.G. Gladyshev, K.A. Podgaetskiy, A.Yu. Andreev, I.V. Yarotskaya, M.A. Ladugin, A.A. Marmalyuk, I.I. Novikov, V.I. Kuchinskii, L.Ya. Karachinsky, A.Yu. Egorov, G.S. Sokolovskii, Phys. Usp., **67** (1), 92 (2024). DOI: 10.3367/UFNe.2023.05.039543.

[3] F. DÁmato, M. Barucci, G. Bianchini, S. Viciani, Opt. Express, **33** (11), 22745 (2025). DOI: 10.1364/OE.558437

[4] K.K. Schwarm, C.L. Strand, V.A. Miller, R.M. Spearrin, Appl. Phys. B, **126** (1), 9 (2020). DOI: 10.1007/s00340-019-7358-x

[5] M. Joharifar, H. Dely, X. Pang, R. Schatz, D. Gacemi, T. Salgals, A. Udalcovs, Y.-T. Sun, Y. Fan, L. Zhang, E. Rodriguez, S. Spolitis, V. Bobrovs, X. Yu, S. Lourdudoss, S. Popov, A. Vasanelli, O. Ozolins, C. Sirtori, J. Lightwave Technol., **41** (4), 1087 (2023). DOI: 10.1109/JLT.2022.3207010

[6] O. Spitz, P. Didier, L. Durupt, D.A. Díaz-Thomas, A.N. Baranov, L. Cerutti, F. Grillot, IEEE J. Sel. Top. Quantum Electron., **28**, 1200109 (2022). DOI: 10.1109/JSTQE.2021.3096316

[7] J. Huang, Z. Shen, Z. Wang, Z. Zhou, Z. Wang, B. Peng, W. Liu, Y. Chen, B. Chen, IEEE Electron. Dev. Lett., **43** (5), 745 (2022). DOI: 10.1109/LED.2022.3163660

[8] Q. Lin, M. Hakl, S. Lepillet, H. Li, J.-F. Lampin, E. Peytavit, S. Barbieri, Optica, **10**, 1700 (2023). DOI: 10.1364/OPTICA.505745

[9] T. Dougakiuchi, N. Akikusa, Sensors, **21**, 5706 (2021). DOI: 10.3390/s21175706

[10] T. Dougakiuchi, A. Ito, M. Hitaka, K. Fujita, M. Yamanishi, Appl. Phys. Lett., **118**, 041101 (2021). DOI: 10.1063/5.0038147

[11] J. Hillbrand, L.M. Krüger, S.D. Cin, H. Knötig, J. Heidrich, A.M. Andrews, G. Strasser, U. Keller, B. Schwarz, Opt. Express, **29**, 5774 (2021). DOI: 10.1364/OE.417976

[12] G. Quinchard, C. Mismer, M. Hakl, J. Pereira, Q. Lin, S. Lepillet, V. Trinité, A. Evirgen, E. Peytavit, J.L. Reverchon, J.F. Lampin, S. Barbieri, A. Delga, Appl. Phys. Lett., **120** (9), 091108 (2022). DOI: 10.1063/5.0078861

[13] B. Schwarz, C.A. Wang, L. Missaggia, T.S. Mansuripur, P. Chevalier, M.K. Connors, D. McNulty, J. Cederberg, G. Strasser, F. Capasso, ACS Photonics, **4**, 1225 (2017). DOI: 10.1021/acsphotonics.7b00133

[14] V.V. Dudelev, D.A. Mikhailov, A.V. Babichev, G.M. Savchenko, S.N. Losev, E.A. Kognovitskaya, A.V. Lyutetskii, S.O. Slipchenko, N.A. Pikhtin, G. Gladyshev, D.V. Denisov, I.I. Novikov, L.Ya. Karachinsky, V.I. Kuchinskii, A.Yu. Egorov, G.S. Sokolovskii, Quantum Electron., **50** (11), 989 (2020). DOI: 10.1070/QEL17396.

[15] G. Marschick, M. David, E. Arigliani, N. Opacak, B. Schwarz, M. Giparakis, A. Delga, M. Lagree, T. Poletti, V. Trinite, A. Evirgen, B. Gerard, G. Ramer, R. Maulini, J. Butet, S. Blaser, A.M. Andrews, G. Strasser, B. Hinkov, Opt. Express, **30**, 40188 (2022). DOI: 10.1364/OE.470615

Translated by EgoTranslating